

**PRACTICAL SUPERCONDUCTOR DEVELOPMENT
FOR ELECTRICAL POWER APPLICATIONS
ARGONNE NATIONAL LABORATORY
QUARTERLY REPORT FOR THE PERIOD ENDING DECEMBER 31, 2001**

This is a multiyear experimental research program that focuses on improving relevant material properties of high- T_c superconductors (HTSs) and developing fabrication methods that can be transferred to industry for production of commercial conductors. The development of teaming relationships through agreements with industrial partners is a key element of the Argonne (ANL) program.

Technical Highlights

The microstructure of $\text{YBa}_2\text{Cu}_3\text{O}_x$ (YBCO) films deposited directly onto silver substrates has been characterized. Doping of YBCO grain boundaries with strontium was shown in some instances to improve transport across the grain boundaries. YBCO rings were tested for possible use in a superconducting shielded core reactor (SSCR), a device under development as a fault-current limiter for power distribution grids. A novel heat treatment increases the critical current density of Bi-2223 conductors by reducing the concentration of nonsuperconducting phases after the first heat treatment. Transmission X-ray diffraction (XRD) measurements have been shown to be beneficial in studying Ag/Bi-2223 composite conductors.

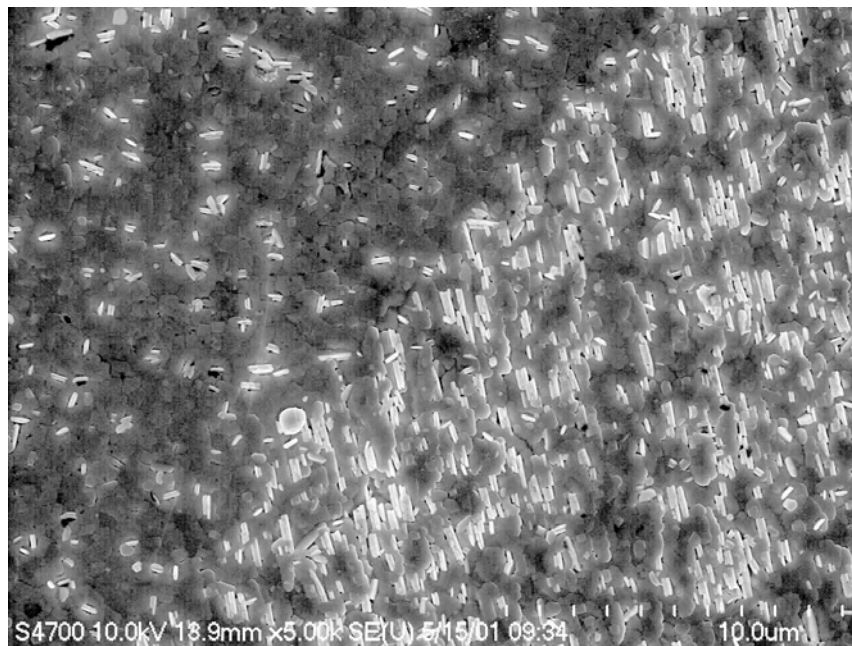
Microstructure of YBCO on Polycrystalline Silver Substrate

We previously [1] described c-axis-oriented YBCO films that were deposited directly on polycrystalline silver substrates by inclined substrate pulsed laser ablation. Films made by this method had a sharp superconducting transition temperature (T_c) with an onset of ≈ 90 K and a transition width of ≈ 2 K. A film that was $0.14 \mu\text{m}$ thick, 5 mm wide, and 10 mm long had a transport critical current density (J_c) of $2.7 \times 10^5 \text{ A/cm}^2$ at 77 K in zero field (using a $1 \mu\text{V/cm}$ criterion). In this reporting period, we characterized the YBCO films by using scanning electron microscopy (SEM), X-ray methods, and Raman spectroscopy.

The surface morphology of the YBCO films was studied by SEM. At low magnification (Fig. 1a), a mosaic of irregularly shaped areas is observed with clear, sharp boundaries between them. In all areas of the film, there are short



(a)



(b)

Fig. 1. Secondary electron images of YBCO films on silver showing sharp borders between different regions of the film.

($\approx 0.5 \mu\text{m}$) rectangular grains that resemble a-axis-oriented grains; however, the orientation of these grains has not been confirmed. A boundary between two areas of the film, seen at higher magnification in Fig. 1b, shows that the darker area appears denser and contains relatively few "a-axis" grains. The brighter area seem less dense and has a higher concentration of "a-axis" grains, all apparently oriented in a particular direction. It is not known at this time how in-plane texture varies among different areas. Energy-dispersive spectroscopy (EDS) of X-rays in the SEM shows no obvious composition difference among the areas.

The morphology of the YBCO film appears to be directly related to that of the silver substrate. This is seen in Fig. 2, which compares the morphology of a YBCO film (Fig. 2a) to that of its silver substrate after removal of the YBCO film (Fig. 2b). Both images show twinning, and in many cases there is direct correspondence between the images. The similarity in size and shape of the grains clearly shows the correlation in morphology between YBCO and silver, and suggests that the microstructure of the YBCO film was influenced by that of the silver substrate.

The XRD pattern of the YBCO film on polycrystalline silver (Fig. 3) consists of sharp and strong peaks, all of which have been identified as YBCO(00 l) peaks. No peaks associated with a-axis orientation appear in this pattern. An Ω -scan of the YBCO(005) peak (Fig. 3b) gave a full-width half-maximum (FWHM) value of 3.8° , indicating good c-axis alignment of the YBCO film. Analysis of the YBCO(103) pole figure (Fig. 3c), however, shows that the diffracted intensity is generally distributed uniformly over the whole $360^\circ \phi$ -angle range, indicating a random in-plane texture. This finding is not surprising considering the polycrystalline nature of the substrate. The XRD pattern for the silver substrates (Fig. 3d) shows roughly equivalent intensities for the (111), (200), (220), and (311) diffraction peaks, indicating that the substrate shows no preferred orientation. Ω -scans for each of these peaks gave a wide distribution of intensity (FWHM = $10\sim 15^\circ$), suggesting a highly random orientation distribution of the silver grains.

Raman spectra were also used to obtain information about microstructure, cation disorder, and second-phase formation such as CuO and BaCuO₂. Figure 4 shows the Raman spectrum of the as-grown YBCO films, which exhibit a strong Raman band at 340 cm^{-1} , along with a weak band centered at $\approx 500 \text{ cm}^{-1}$. The spectrum was recorded in the xx/yy mode, in which the laser excitation and observation directions were perpendicular to the substrate. In this configuration, a stoichiometric YBCO film with perfect c-axis-orientation should exhibit only one band at $\approx 340 \text{ cm}^{-1}$ over the range of 200 to 800 cm^{-1} . The weak band at $\approx 500 \text{ cm}^{-1}$ may indicate some degree of c-axis misalignment in the YBCO film

(a)

(b)

Fig. 2. SEM images of (a) YBCO film and (b) Ag substrate at same area after YBCO film was removed from substrate. Morphology correlation between film and substrate is clearly seen.

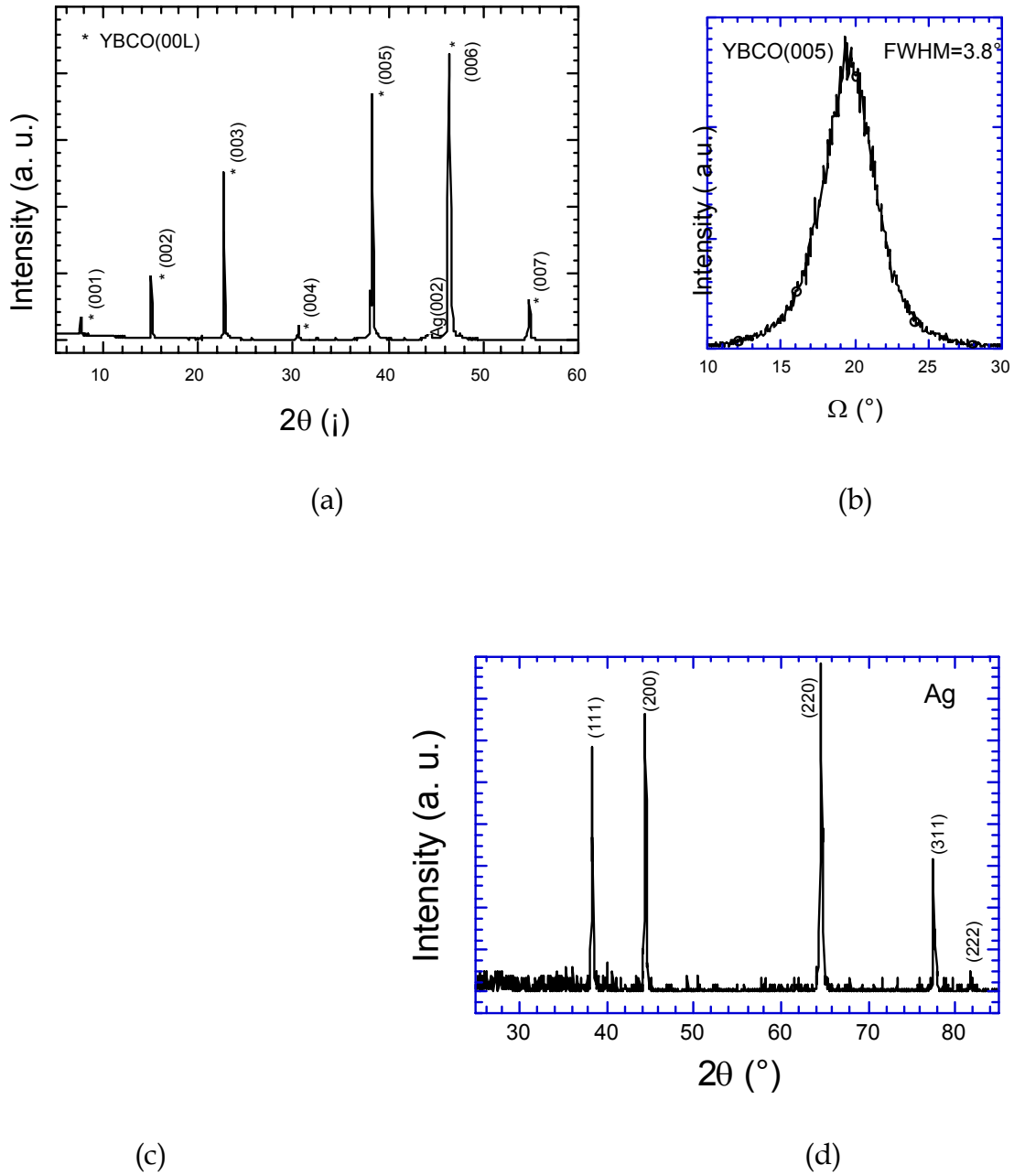


Fig. 3. X-ray diffraction patterns of YBCO/Ag films: (a) 2θ -scan, (b) Ω -scan of YBCO(005), (c) pole-figure of YBCO(103), and (d) 2θ -scan of Ag substrates.

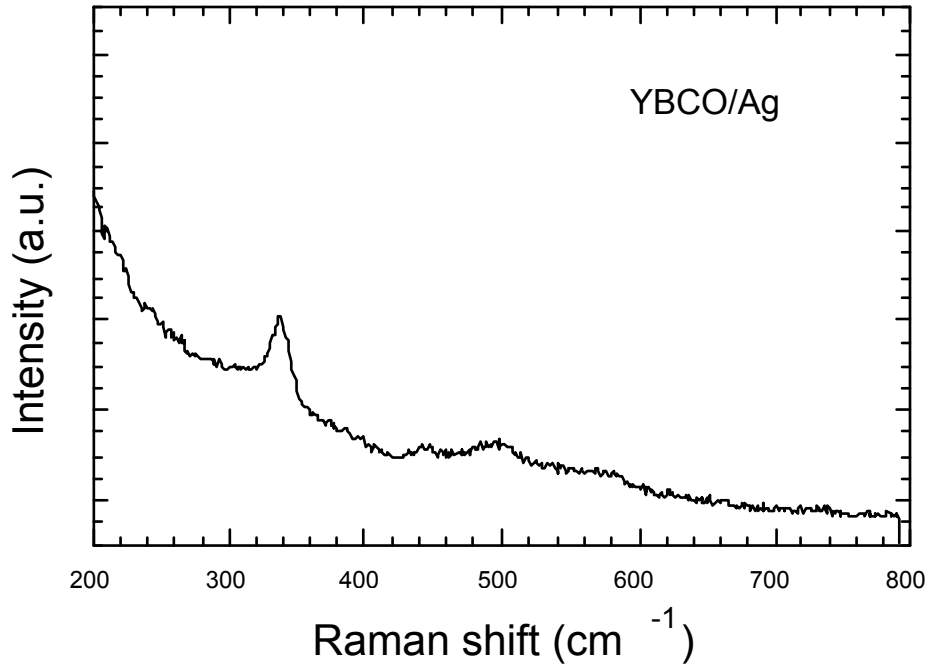


Fig. 4. Raman spectrum of YBCO film grown on polycrystalline silver substrate.

[2-3], but may also be attributed to some extent to a lack of in-plane texture. The absence of other peaks suggests that the YBCO film has a stoichiometric composition.

Effect of Dopants on Grain Boundary Transport

The effect of Sr doping on grain boundary supercurrent transport in YBCO was investigated as part of a larger effort to study the effects of various grain boundary dopants on supercurrent transport across grain boundaries. The investigation was stimulated by previously reported studies of Ca doping in grain boundaries of thin-film or coated-conductor samples (e.g., Mannhart et al.), in which significant improvement in J_c was observed. We observed similar improvements in grain boundary transport in bulk samples when Ca was diffused into the grain boundaries.

For this study, grain boundary J_c values were measured with a new technique that exploits Superconductor Quantum Interference Device (SQUID) measurements on ring samples. Well-controlled [001] tilt grain boundaries with desired misorientation angles are grown in bulk melt-textured YBCO by a dual

seeding technique. Typical misorientation angles are $\approx 20^\circ$. This nondestructive technique and the use of bulk samples allows for extensive sample reprocessing so that diffusion and oxygenation effects can be systematically studied. Film samples are probably not sufficiently robust for such studies. Dopants and processing methods that improve the grain boundary J_c values of bulk YBCO rings will be investigated in coated-conductor samples with the goal of minimizing energy losses across grain boundaries.

Our results indicate that Sr doping of grain boundaries does not appear to generally improve grain boundary transport, although improvement can apparently be achieved under certain processing conditions. Sr doping appears to significantly improve grain boundaries that have very low transport capability. With such grain boundaries, improvements in J_c by a factor of 5 or more were observed at 77 K. Even samples that initially gave no grain boundary transport showed a substantial J_c after Sr treatment (similar treatments with no Sr showed no significant improvement). However, for high-quality bulk grain boundaries (i.e., those with J_c levels in the upper range of values in the standard plots of J_c vs. misorientation angle), Sr treatment does not appear to be universally beneficial.

Most of our Sr diffusion studies were conducted with heat treatments at 970°C in the presence of SrCO_3 . It appears that Sr thoroughly decorates the grain boundaries, but a complex aging process apparently occurs during the oxygenation step. Grain boundary oxygenation can be very rapid (even 2 h at 450°C in O_2 seems sufficient to oxygenate a grain boundary that extends across a sample with a $1 \times 1 \text{ mm}^2$ cross section). For Sr-doped bicrystal rings, J_c is quite high after only a few hours of oxygenation, being comparable to untreated grain boundaries (i.e., those without Sr). After longer oxygen treatments, however, J_c in Sr-doped bicrystals typically declines and saturates at 20 to 50% of the peak value. On the other hand, dense polycrystalline samples show, with remarkable robustness, a small ($\approx 30\%$) improvement in J_c measured at 77 K when given the Sr treatment and an extended ($\approx 24 \text{ h}$) oxygenation.

The time evolution of J_c during the oxygenation of Sr-treated samples suggests that competing processes are at work, one process tending to increase J_c , while the other decreases J_c . The characteristic times for these processes are different, each with its own temperature dependence. Preliminary studies indicate that J_c can be optimized by selecting the oxygenation conditions so that the positive process dominates. For example, we have observed that the J_c of a high-quality undoped grain boundary (maximum J_c obtained with 450°C oxygenation) can be increased moderately ($\approx 30\%$) with Sr treatment followed by oxygenation at low temperature (350°C).

These results suggest that the behavior of Sr in grain boundaries is highly complex. One possible cause for this complex behavior is that the YBCO phase decomposes during preparations at ambient pressure when the Sr concentration exceeds a value of $x \approx 1$ in the system $\text{YBa}_{2-x}\text{Sr}_x\text{Cu}_3\text{O}_{7-x}$ [4]. At the grain boundary interface, it is possible that the Sr concentration is high enough for phase decomposition to occur, perhaps influenced by the level and kinetics of oxygenation. The results also suggest that optimized Sr-diffusion and oxygenation treatments might lead to significant improvements in grain boundary supercurrent transport. Similarly, optimized heat treatments with other dopants could also improve grain boundary transport.

YBCO Rings for Superconducting Shielded Core Reactors

A project is underway to examine the use of large YBCO ring and tube structures in a superconducting shielded core reactor (SSCR), a device under development as a fault-current limiter for electric power distribution grids. Intended for large-scale application, the SCCR has a design temperature of 77 K so low-cost refrigeration can be employed. Previous work includes the construction of a prototype BSCCO-based device through a CRADA with the S&C Electric Company, an electrical switchgear manufacturer in Chicago [5]. Although the device functioned properly, various material-related limitations were discovered. A joint decision was reached to try substitution of oriented-grain YBCO rings in place of the BSCCO components.

Rings available from Superconducting Components Inc., of Columbus, Ohio, were tested for this application. Induced currents above 50 kA were achieved, and a simple fault-current limiter was demonstrated at that current level [6]. In the course of this work, transient magnetic field effects were studied by applying pulsed magnetic fields with rise times on the order of 10 ms. Because these devices are intended for use in a 60 Hz power distribution grid, a rise time of 4-5 ms is needed to duplicate the first quarter-cycle of a 60 Hz sine wave under overload conditions. In order to make these faster measurements, various improvements were made to an existing experimental apparatus, as shown in Fig. 5.

A copper-wire drive coil impresses a pulsed magnetic field on the outer surface of the superconducting ring that is being tested. The current pulser contains a large capacitor bank and a set of custom-designed field effect transistor (FET) switch banks that allow short-duration current pulses to be manipulated. Current pulses of 500 A at 100 V, representing a power of 50 kW, can be readily controlled. Pulses up to about 150 kW can be achieved under more limited control. The digital data acquisition system can digitize multiple

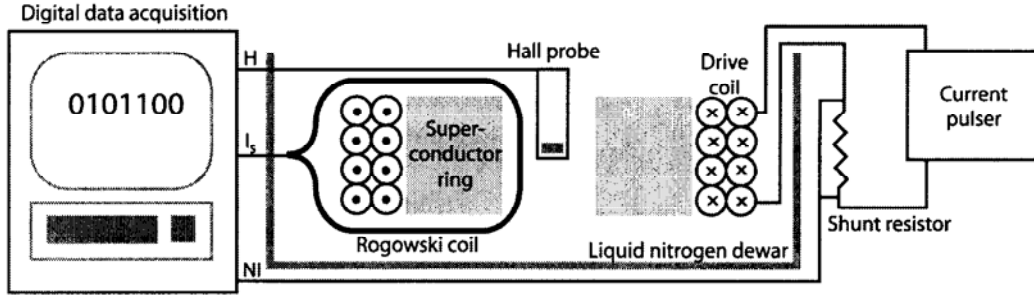


Fig. 5. Schematic diagram of experimental apparatus.

inputs at 16-bit accuracy with a cycle time of 200 μ s. One input, marked “NI,” records the voltage from a precision shunt placed in series with the drive coil. The shunt measures the drive current “I” as a function of time, but the drive coil has “N” turns (usually 60-600), so if the inductive coupling between the ring and drive coil is strong, the induced current will be “NI.” A second input measures the voltage from a type of current transformer called a Rogowski coil. Changes in any current threading the coil produce a voltage in the coil through Faraday’s Law, $V_{\text{induced}} = dI/dt$. Integrating this produces the value of the current threading the ring as a function of time. Because both the drive coil and superconducting ring thread the Rogowski coil, this variable is the sum of the two currents. The drive coil current is already known through measurement of the shunt and can be subtracted to produce the induced current in the superconducting ring, I_s . The magnetic field in the center of the ring is also recorded as a function of time.

The initial analysis was performed on a set of high-quality YBCO rings available from another research project on site. These rings were initially developed for a detailed analysis of the effects of grain boundaries on critical current, the control of which is a key problem in the development of successful SSCR devices [7]. The best of these rings have critical current densities of ≈ 20 kA/cm² at 77 K, a value that is appropriate for power grid applications. The size (typically 2.7 cm OD) and cross section (0.5 cm²) are suitable for testing, but are below those needed for prototype development by a factor of about 4. The rings are highly uniform in their magnetic properties, a feature that is of considerable value in this study. Because the magnetic flux penetrates along radial directions around the entire circumference of the ring, variation in magnetic properties around the ring will have the effect of averaging out millisecond-scale phenomena in each segment. Only when all the segments respond with similar flux dynamics can the millisecond-scale behavior of the structure be understood.

Figure 6 shows the behavior of one ring just before magnetic flux penetration. A pulse of 23 kA-turns has been applied, with its magnitude peaking at 3 ms. The induced superconducting current I_s peaks at 9,500 A. This is graphed as a negative current, because it is opposed in direction to the drive current, NI. The superconducting ring excludes much of the applied magnetic field from the center of the ring, but does allow the field to peak there at about 5.5 ms. If the system is driven with a slightly stronger pulse (25 kA-turns), it approaches the threshold of penetration, as shown in Fig. 7. Although the current function has hardly changed, the behavior of the magnetic field at the center of the ring shows the onset of penetration and the temporal characteristics of magnetic diffusion. A further increase to 27 kA-turns, shown in Fig. 8, produces a rapid and very uniform penetration in 3-4 ms. After this, a period of ≈ 5 ms follows, during which the induced current in the superconductor exhibits complex behavior and apparently reverses in direction. Further work is planned to measure this post-penetration behavior under various design conditions. Explanation of the observed phenomena should enable their manipulation and resultant performance improvements in SSCRs.

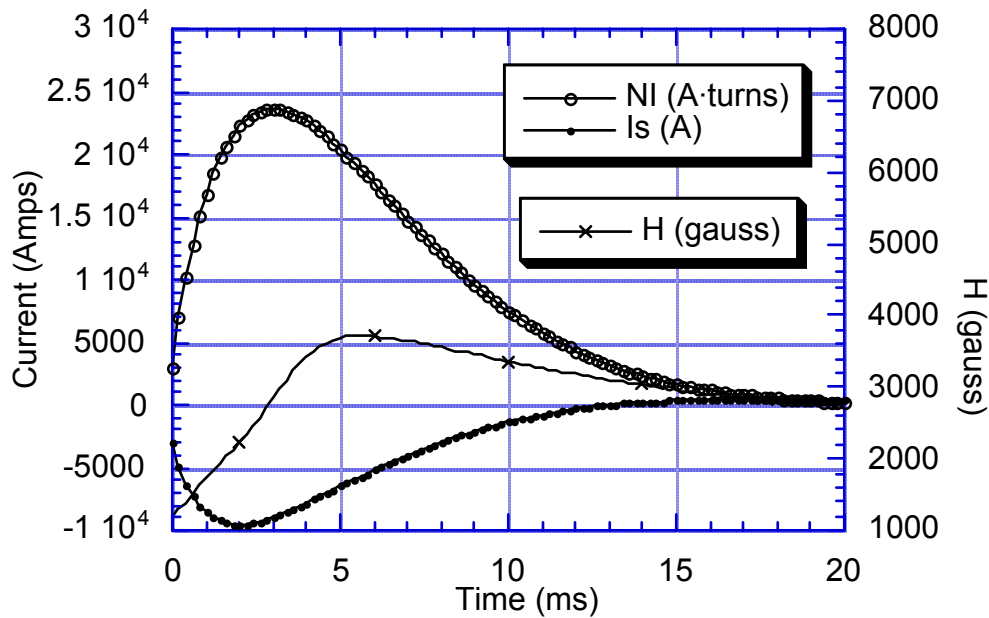


Fig. 6. YBCO ring under pulsed magnetic field conditions, approaching penetration.

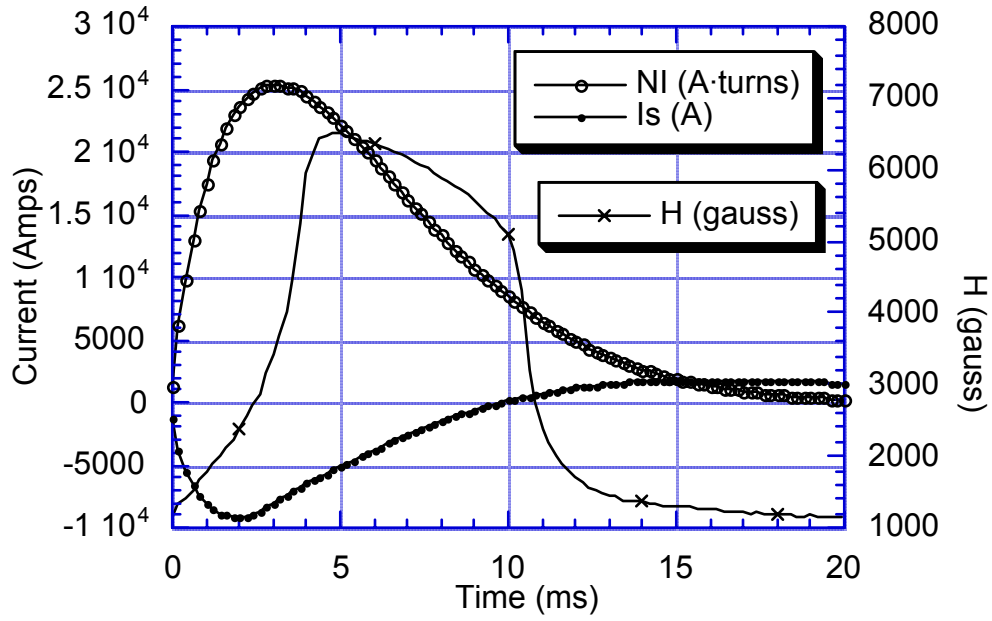


Fig. 7. YBCO ring under pulsed magnetic field conditions, on penetration threshold.

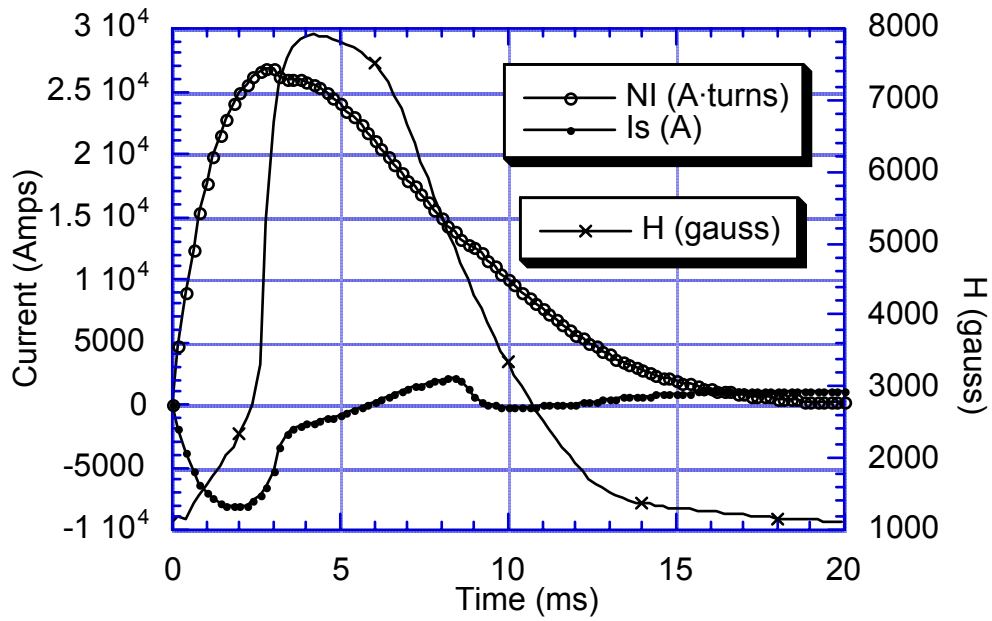


Fig. 8. YBCO ring under pulsed magnetic field conditions, after penetration.

Dissipation of Nonsuperconducting Second Phases (NSPs) in Multifilament-Type Ag/Bi-2223 Composite Conductors

In a previous quarterly report, we presented results that showed how temperature and partial pressure of oxygen (pO_2) influence phase evolution and microstructure development during the first heat treatment (HT1) of powder-in-tube-type Ag/Bi-2223 composite conductor. These results revealed that for a given pO_2 in the range of pO_2 values where the Bi-2223 phase is stable (nominally 0.04 to 0.21 atm), there is an onset temperature for the growth of robust Bi-2223 grain colonies (a desirable effect) and another onset temperature for the persistent formation of large NSPs (an undesirable effect). These two temperatures have been termed the grain-growth-takeoff temperature (GGTT) and the second-phase-takeoff temperature (SPTT), respectively. The results also showed that NSP composition varies significantly with pO_2 and temperature, from a CuO-dominated mix at low pO_2 to a $(Ca,Sr)_2CuO_3$ -dominated mix at intermediate pO_2 to a $(Ca,Sr)_{14}Cu_{24}O_{41}$ -dominated mix at the highest pO_2 . Based on these observations, we showed that the constituent species of the NSP mix (within the range of pO_2 levels and temperatures where the Bi-2223 phase is stable) could be manipulated so that the size and number of residual NSPs after HT1 are significantly reduced. This is done by sliding along the lower bound of the GGTT and SPTT curves between 0.04 atm O_2 and 0.21 atm O_2 , as reported previously [8]. The principal objective of this sliding heat treatment method (hereinafter called thermal slide heat treatment, or TSHT) is to minimize the damage to Bi-2223 grain colonies that is caused by residual NSPs when the Ag/Bi-2223 conductor is subjected to intermediate size reduction following HT1.

Over the past year, we have carried out an extensive series of tests of the TSHT method in collaboration with American Superconductor (AMSC). In this test series, multifilament-type Ag/Bi-2223 wires were subjected to a variety of TSHTs and conventional HT1s at ANL, then sent to AMSC for intermediate size reduction and final heat treatment. Following the final heat treatment, the critical current density of each specimen was measured by a transport method. In addition, a portion of each post-HT1 specimen was examined at ANL by SEM/EDS to determine the area fraction and size distribution of NSPs prior to the intermediate size reduction step. Figure 9 shows representative SEM images of specimens that were subjected to standard (single pO_2 /temperature set point) HT1 and to TSHT-type HT1s. The reduced NSP content in the TSHT specimens is clearly illustrated in these images (NSPs are the dark spotted areas in each filament).

In Fig. 10, we show a plot that compares the area% of NSP after HT1 with the corresponding critical current density (J_c) in the fully processed state for a typical set of specimens from this study. A key result here is the precipitous

increase in J_c for specimens with <8 area% NSP when compared to J_c for specimens with >13 area% NSP. This observation lends considerable support to the notion that at some level the NSPs remaining after HT1 can lead to a degradation of the J_c of fully heat-treated Ag/Bi-2223 wires. We are currently examining the data for specimens with <8 area% NSP to determine the extent to which other phase and microstructural characteristics of post-HT1 specimens have an influence on the J_c of fully processed wire.

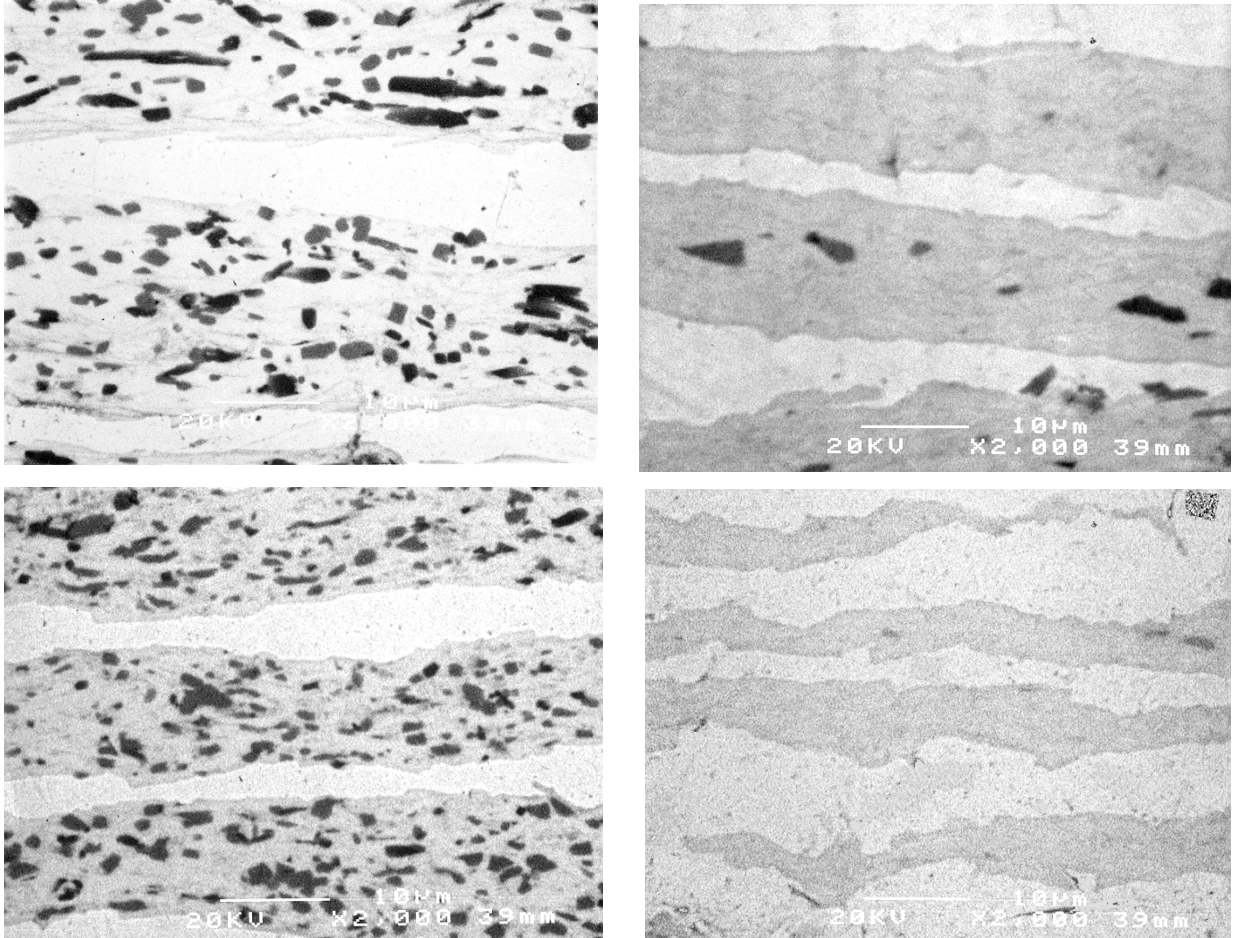


Fig. 9. Transverse-section SEM images of representative Ag/Bi-2223 multifilament wire specimens after standard (single pO_2 /temperature set point) first heat treatment (left two images) and after optimized TSHT-type first heat treatment (right two images). Dark spotted areas in filaments are alkaline earth cuprate NSPs.

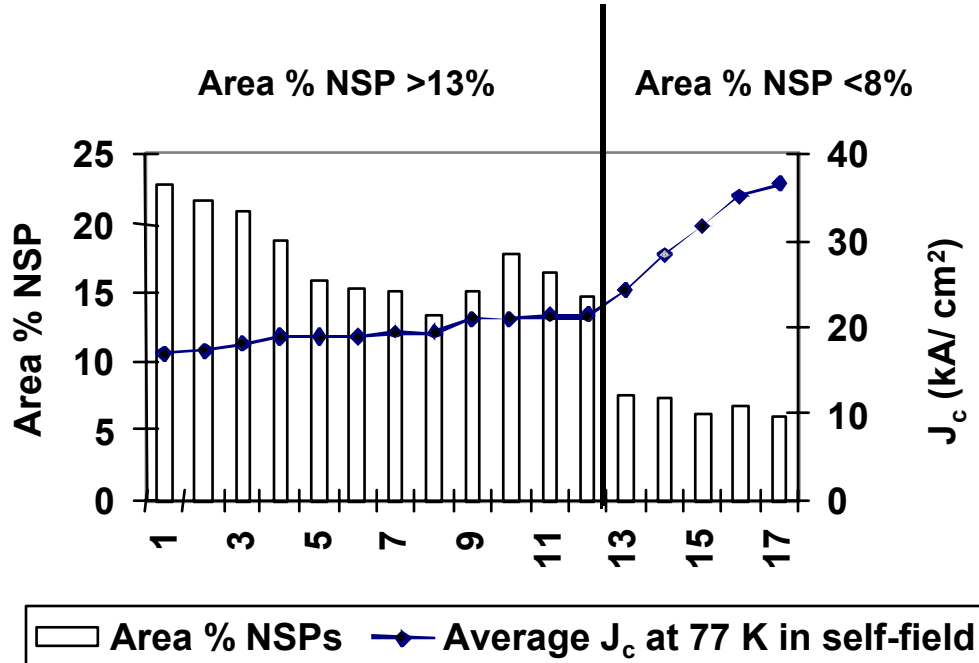


Fig. 10. Bar graph showing post-first-heat-treatment area% NSP for Ag/Bi-2223 multifilament wire specimens subsequently subjected to intermediate size reduction and final heat treatment. Specimens are arranged in order of increasing J_c (from left to right) of fully processed specimen.

Transmission X-ray Diffraction Measurements on Multifilament Ag/Bi-2223 Composite Conductor

The central step in the powder-in-tube process for Ag/Bi-2223 composite conductors is the heat treatment that transforms the ceramic powder mixture in the precursor billet into the superconducting Bi-2223 phase. Monitoring of this process as a function of process variables (e.g., time, temperature, and pO_2) requires direct examination of the samples. The primary methods employed in virtually all cases today are X-ray diffraction (with a laboratory source) and SEM coupled with EDS. With both of these methods, the sample must be sectioned and the silver polished away to expose the superconducting ceramic cores, i.e., both methods require destructive sectioning of the sample. In addition, during heat treatment of Ag/Bi-2223 composites, the Bi-2223 phase forms in a grain colony microstructure with the crystallographic c-axis perpendicular to the rolling direction. As a consequence of this texturing and the measurement configuration for the conventional theta/two-theta scan, the [00L] reflections of the layered cuprate phases (Bi-2212 and Bi-2223) dominate the diffraction pattern. With the dominance of the Bi-2212 and Bi-2223 peaks, it is difficult to detect impurity phases such as the 2201 phase, certain alkaline earth cuprates,

and a lead-rich/copper-deficient cuprate known as the “3221” phase, when using the conventional x-ray diffraction (XRD) approach.

As an alternative to the conventional XRD method, we are investigating transmission XRD at X-ray energies high enough to fully penetrate the silver-sheathed composites. This avoids the need to abrade away the silver and also, in principle, avoids the need to section long lengths of composite wire. We have found that this can be done very effectively by working at 25 keV (0.49594 Å), an energy that lies just below the silver $K\alpha$ edge. Using this technique, we have determined the bulk second-phase content of as-rolled, partially heat-treated, and fully heat-treated Ag/Bi-2223 specimens without any damage to the specimen itself. This allows us to investigate the same specimen at progressive stages of the deformation/heat treatment process.

The fully processed 51-filament Ag/Bi-2223 composite wires investigated in this study were provided by AMSC. Measurements were made on the Materials Research Collaborative Access Team (MR-CAT) insertion device beamline at ANL’s Advanced Photon Source by using an eight-circle Huber diffractometer. The beam spot on the sample was slitted to a 2 by 1 mm rectangle. Patterns were recorded at $\approx 1^\circ/\text{minute}$.

Figure 11 compares XRD scans for a typical Ag/Bi-2223 specimen that were obtained by the conventional laboratory-source method (Cu- $K\alpha$) and the synchrotron-based transmission method. For comparison, the Cu- $K\alpha$ data were recomputed to the 0.49594 Å wavelength used in the transmission experiment. Pattern (a) in Fig. 11, obtained with the laboratory-source configuration, is dominated by the [00L] reflections of Bi-2223, with only trace evidence of the 3221 phase (near two-theta = 10°). Pattern (b) in Fig. 11, obtained using the transmission XRD technique, contains identifiable diffraction lines for at least four other phases in addition to the Bi-2223 phase. It is noteworthy that in pattern (b), the [00L] reflections of Bi-2223 are not observed. This is because the X-ray beam is imposed on the Ag/Bi-2223 wire at a right angle to the rolling direction and is therefore parallel to the crystallographic c-axis of the Bi-2223 grain colonies. Instead of the [00L] reflections of Bi-2223, the pattern contains mainly [10L] and [11L] reflections of the Bi-2223, Bi-2212, and Bi-2201 phases, plus at least four diffraction lines of the 3221 phase, and a low-angle reflection ($\approx 4.3^\circ$) that may be due to either the $(\text{Ca,Sr})_{14}\text{Cu}_{24}\text{O}_{41}$ alkaline earth cuprate or layered-phase intergrowth boundaries. Also, the [200], [202], and [220] reflections of Bi-2223 appear with considerable intensity, and like the two silver diffraction lines, are actually off-scale in pattern b due to detector saturation. (Beam attenuation is required to bring the intensities of these two lines back into the dynamic range of the detector.)

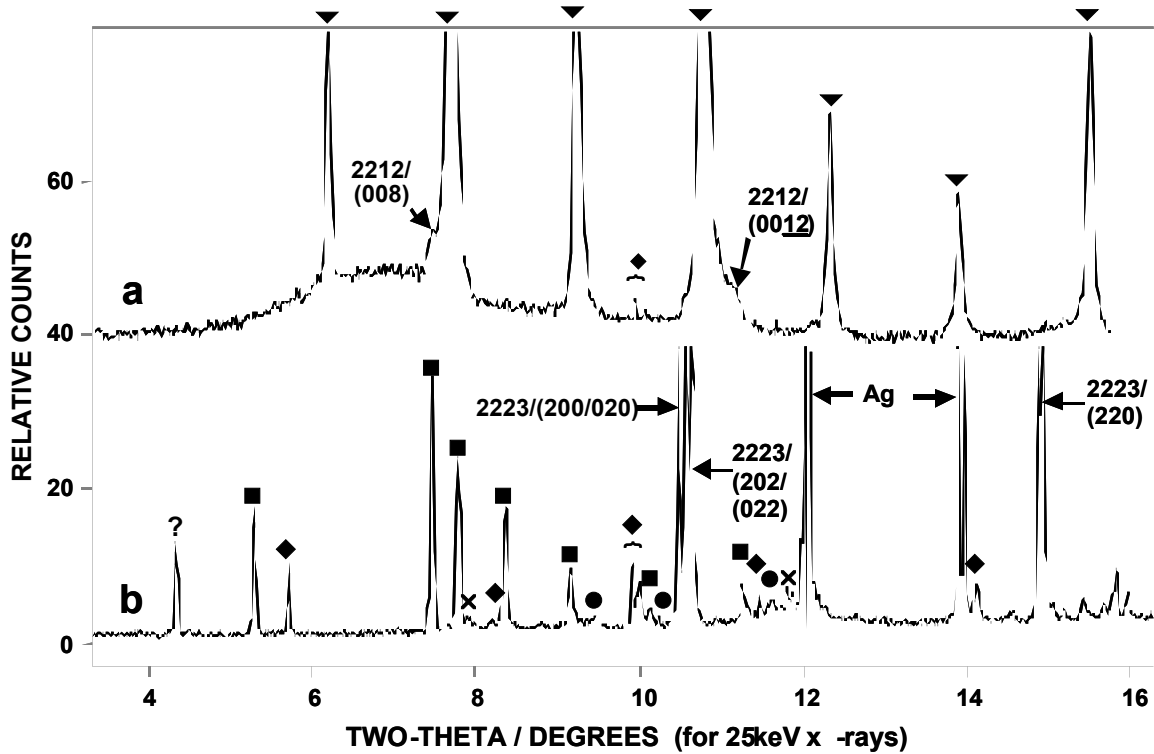


Fig. 11. Pattern **a** is a theta/two-theta diffraction pattern from an abraded Ag/Bi-2223 composite wire taken with a Cu-K α laboratory source and recomputed to a wavelength of 0.49594 Å. Pattern **b** is a transmission-type two-theta diffraction pattern of the same composite wire recorded using 0.49594 Å X-rays at the MR-CAT insertion device beamline. ∇ = [00L] of Bi-2223, \blacksquare = [10L] and [11L] of Bi-2223, \times = [11L] of Bi-2212, \bullet = [11L] of Bi-2201, and \blacklozenge = [HKL] of the 3221 phase. Beyond two-theta = 15°, the pattern consists of a near continuum of Bi-2223, Bi-2212, and Bi-2201 diffraction lines.

Clearly, the 25 keV transmission XRD technique provides considerably more information about impurity phases in Ag/Bi-2223 composites than does the conventional laboratory-source method. This is due in large part to the full transverse penetration of the Bi-2223 filaments achieved with the transmission XRD method. Also, the absence of the Bi-2223 [00L] reflections in the transmission two-theta configuration is a testimony to the quality of the preferential Bi-2223 a-b plane alignment achieved by the powder-in-tube process. We are currently investigating the prospects for on-line transmission XRD of Ag/Bi-2223 composite wire with an industrial-scale X-ray source equipped with a silver anode.

References

1. Practical Superconductor Development for Electrical Power Applications, Argonne National Laboratory, Quarterly Report for July-Sept. 2001.
2. J. R. Ferraro and V. A. Maroni, *Appl. Spectrosc.*, **44**, pp. 351-366 (1990).
3. G. Gibson, L. F. Cohen, R. G. Humphreys, and J. L. MacManus-Driscoll, *Physica C*, **333**, pp. 139-145 (2000).
4. B. Veal, et al., *Appl. Phys. Lett*, **51**, 279 (1987).
5. M. G. Ennis, et al., "Fault Current Limiter – Predominantly Resistive Behavior of a BSCCO-Shielded-Core Reactor," *IEEE Transactions on Applied Superconductivity*, **11**, 2050 (2001).
6. T. R. Askew and Y. S. Cha, "Transient Response of 50 KiloAmp YBCO Rings and Ring Pairs to Pulsed Magnetic Fields," *IEEE Transactions on Applied Superconductivity*, **11**, 3947 (2001).
7. H. Claus, et al., "Critical Current Across Grain Boundaries in Melt-Textured YBCO Rings," *Physical Review B*, **64**, 144507 (2001).
8. Practical Superconductor Development for Electrical Power Applications, Argonne National Laboratory, Quarterly Report for Jan.-March 2000.

Interactions

Dr. Beihai Ma received the Young Investigator Award on Dec. 13, 2001 in Washington, DC, from the Office of Energy Efficiency and Renewable Energy, Office of Power Technologies 2000 Research and Development Awards.

Balu Balachandran reviewed the IGC-DOE Coated Conductor Program at IGC-SuperPower on Oct. 9, 2001, in Schenectady, NY.

Balu Balachandran attended the post-peer review meeting in Washington, DC, on Oct. 12, 2001.

Balu Balachandran visited Los Alamos National Laboratory and discussed ANL-LANL collaborative work there on Oct. 19, 2001.

Balu Balachandran attended the Air Force Office of Scientific Research Coated Conductor review at Stanford University, Oct. 22-23, 2001.

Balu Balachandran attended the PAC RIM IV conference in Hawaii and presented a talk on coated conductors on Nov. 5-6, 2001.

Balu Balachandran held discussions with DOE program managers in Washington DC, on Nov. 9, 2001.

Beihai Ma and Balu Balachandran visited Universal Energy Systems, Inc., Dayton, OH, and discussed our collaboration in the area of inclined substrate deposition on Nov. 19, 2001.

Vic Maroni, Dean Miller, and Balu Balachandran attended the MRS Fall Meeting, Boston, Nov. 26-30, 2001.

Vic Maroni attended a Wire Development Group Meeting at American Superconductor Corp., Westborough, MA, Nov. 30, 2001.

Beihai Ma and Vic Maroni attended the 10th U.S.-Japan Workshop on High-T_c Superconductors, Santa Fe, NM, Dec. 2-5, 2001.

Publications and Presentations

Published or presented:

Y. A. Jee, M. Li, B. Ma, V. A. Maroni, B. L. Fisher, and U. Balachandran, Comparison of Texture Development and Superconducting Properties of YBa₂Cu₃O_x Thin Films Prepared by TFA and PLD Processes, *Physica C*, Vol. 354/4, pp. 297-303 (2001).

K. Salama (Texas Center for Superconductivity); S. P. Athur, and U. Balachandran, Texturing of REBCO Using Temperature Gradient, *Physica C* 357-360 (2001) 11-19.

J. R. Hull, Energy Storage Systems, Chapter 9.5 in "Properties, Processing, and Applications of YBCO and Related Materials," eds. W. Lo and A. M. Campbell, IEE Books, Stevenage, UK (2001).

J. R. Hull, Superconducting Bearings, Chapter 9.4 in "Properties, Processing, and Applications of YBCO and Related Materials," eds. W. Lo and A. M. Campbell, IEE Books, Stevenage, UK (2001).

M. Li, B. Ma, Y. A. Jee, B. L. Fisher, and U. Balachandran, Structural and Electrical Properties of Biaxially Textured $\text{YBa}_2\text{Cu}_3\text{O}_{7-x}$ Thin Films on Buffered Ni-Based Alloy Substrates, *Mat. Res. Soc. Symp. Proc. Vol. 659, High-Temperature Superconductors -- Crystal Chemistry, Processing and Properties*, pp. II10.2.1-2.6 (2001), eds. U. Balachandran, H. C. Freyhardt, T. Izumi, and D. C. Larbalestier.

Y. A. Jee, B. Ma, M. Li, B. L. Fisher, and U. Balachandran, Texture Formation and Superconducting Properties of $\text{YBa}_2\text{Cu}_3\text{O}_x$ Thin Films Prepared by Solution Process on LaAlO_3 Single Crystals, *Mat. Res. Soc. Symp. Proc. Vol. 659, High-Temperature Superconductors -- Crystal Chemistry, Processing and Properties*, pp. II9.17.1-17.6 (2001), eds. U. Balachandran, H. C. Freyhardt, T. Izumi, and D. C. Larbalestier.

T. M. Mulcahy, J. R. Hull, K. L. Uherka, R. A. Abboud, and J. Juna, Test Results of 2-kWh Flywheel Using Passive PM and HTS Bearings, *IEEE Trans. on Applied Superconductivity*, **11**(1), 1729-1732 (2001).

Y. S. Cha and T. R. Askew, Transient Characteristics of a High- T_c Superconductor Tube Subjected to Internal and External Magnetic Fields, *IEEE Trans. on Applied Superconductivity*, **11**(1), 2458-2488 (2001).

V. Selvamanickam, G. Carota, M. Funk, N. Vo, P. Haldar, U. Balachandran, M. Chudzik, P. Arendt, J. R. Grovesw, R. DePaula, and B. Newnam, High-Current Y-Ba-Cu-O-Coated Conductor Using Metal Organic Chemical-Vapor Deposition and Ion-Beam-Assisted Deposition, *IEEE Trans. on Applied Superconductivity*, **11**(1), 3379-3381 (2001).

T. R. Askew and Y. S. Cha, Transient Response of 50-KiloAmp YBCO Rings and Ring Pairs to Pulsed Magnetic Fields, *IEEE Trans. on Applied Superconductivity*, **11**(1), 3947-3950 (2001).

U. Balachandran, M. Li, R. E. Koritala, B. L. Fisher, and B. Ma, Development of YBCO-Coated Conductors for Electric Power Applications, *Proc. 5th European Conf. on Applied Superconductivity, Copenhagen, Denmark, Aug. 26-30, 2001*.

U. Balachandran, M. Li, R. E. Koritala, B. L. Fisher, and B. Ma, Development of YBCO-Coated Conductors for Electric Power Applications, *PAC RIM IV Conference, Maui, Hawaii, Nov. 5-6, 2001*.

U. Balachandran, B. Ma, M. Li, R. E. Koritala, B. L. Fisher, R. A. Erck, and S. E. Dorris, Fabrication by Inclined-Substrate Deposition of Biaxially Textured Buffer Layer for Coated Conductors, invited paper presented at the Fall 2001 Mtg. of the Materials Research Society, Boston, Nov. 25-29, 2001.

Y. L. Tang, D. J. Miller, B. Ma, R. E. Koritala, and U. Balachandran, Structure Characteristics of ISD Coated Conductors, paper presented at the Fall 2001 Mtg. of the Materials Research Society, Boston, Nov. 25-29, 2001.

B. Ma, M. Li, B. L. Fisher, R. E. Koritala, and U. Balachandran, Inclined-Substrate Deposition of Biaxially Aligned Template Films for YBCO-Coated Conductors, Abstract presented at 10th US-Japan Workshop on High- T_c Superconductors, Santa Fe, NM, Dec. 2-5, 2001.

Submitted:

B. Ma, M. Li, R. E. Koritala, B. L. Fisher, S. E. Dorris, V. A. Maroni, D. J. Miller, and U. Balachandran, Direct Deposition of YBCO on Polished Ag Substrates by Pulsed Laser Deposition, submitted to Physica C (Oct. 2001).

K. E. Gray, The Phenomenology of High-Temperature Superconductive Materials, paper submitted to Space Technology and Applications International Forum (STAIF-2002), 19th Symp. On Space Nuclear Power and Propulsion, Albuquerque, Feb. 3-7, 2002.

B. Ma, M. Li, B. L. Fisher, and U. Balachandran, Epitaxial Growth of YBCO Films on Magnesium Oxide Substrates, abstract to be presented at the 104th Ann. Mtg. & Exposition of the American Ceramic Society, St. Louis, MO, April 28-May 1, 2002.

J. H. Cheon and J. P. Singh, Residual Stress and Strain Tolerance of YBCO-Coated Conductors, abstract to be presented at the 104th Ann. Mtg. & Exposition of the American Ceramic Society, St. Louis, MO, April 28-May 1, 2002.

T. P. Weber, B. Ma, U. Balachandran, and M. McNallan (Univ. of IL at Chicago), Ion-Beam Assisted Deposition of Magnesium Oxide Films for Coated Conductors, abstract to be presented at the 104th Ann. Mtg. & Exposition of the American Ceramic Society, St. Louis, MO, April 28-May 1, 2002.

M. Li, B. Ma, R. E. Koritala, B. L. Fisher, and U. Balachandran, Inclined Substrate Pulsed Laser Deposition of YBCO Thin Films on Polycrystalline Ag Substrates, abstract to be presented at the 104th Ann. Mtg. & Exposition of the American Ceramic Society, St. Louis, MO, April 28-May 1, 2002.

1998-2001 Patents

Method of manufacturing a high temperature superconductor with improved transport properties

Uthamalingam Balachandran, Richard Siegel, and Thomas Askew

U.S. Patent No. 6,191,075 (February 20, 2001).

Method and apparatus for measuring gravitational acceleration utilizing a high temperature superconducting bearing

John R. Hull

U.S. Patent 6,079,267 (June 27, 2000).

Engineered flux pinning centers in BSCCO, TBCCO and Y-123 superconductors

Kenneth C. Goretta, Michael T. Lanagan, Jieguang Hu, Dean J. Miller, Suvankar Sengupta, John C. Parker, U. Balachandran, Donglu Shi, and Richard W. Siegel

U.S. Patent 5,929,001 (July 27, 1999).

Passive fault current limiting device

Daniel J. Evans and Yung S. Cha

U.S. Patent 5,892,644 (April 6, 1999).

Automatic HTS force measurement instrument
Scott T. Sanders and Ralph C. Niemann
U.S. Patent 5,889,397 (March 30, 1999).

Method and etchant to join Ag-clad BSCCO superconducting tape
Uthamalingam Balachandran, A. N. Iyer, and J. Y. Huang
U.S. Patent 5,882,536 (March 16, 1999).

Elongated Bi-based superconductors made by freeze dried conducting powders
Uthamalingam Balachandran, Milan Lelovic, and Nicholas G. Eror
U.S. Patent 5,874,384 (Feb. 23, 1999).

Thin-film seeds for melt processing textured superconductors for practical applications
Boyd W. Veal, Arvydas Paulikas, Uthamalingam Balachandran, and Wei Zhong
U.S. Patent 5,869,431 (Feb. 9, 1999).

Superconductor composite
Stephen E. Dorris, Dominick A. Burlone, and Carol W. Morgan
U.S. Patent 5,866,515 (Feb. 2, 1999).

Surface texturing of superconductors by controlled oxygen pressure
Nan Chen, Kenneth C. Goretta, and Stephen E. Dorris
U.S. Patent 5,856,277 (Jan. 5, 1999).

Method for synthesizing and sinter-forging Bi-Sr-Ca-Cu-O superconducting bars
Nan Chen, Kenneth C. Goretta, and Michael T. Lanagan
U.S. Patent 5,821,201 (Oct. 13, 1998).

Mixed- μ superconducting bearings
John R. Hull and Thomas M. Mulcahy
U.S. Patent 5,722,303 (March 3, 1998).